ACS APPLIED MATERIALS & INTERFACES

Article

Gold Nanoparticles Deposited Polyaniline-TiO2 Nanotube for Surface Plasmon Resonance Enhanced Photoelectrochemical Biosensing

Jie Zhu, Xiaohe Huo, Xiaoqiang Liu, and Huangxian Ju

ACS Appl. Mater. Interfaces, **Just Accepted Manuscript** • DOI: 10.1021/acsami.5b08837 • Publication Date (Web): 17 Dec 2015

ACS Publications

ACS Applied Materials & Interfaces is published by the American Chemical Society.
1155 Sixteenth Street N.W., Washington, DC 20036

Gold Nanoparticles Deposited Polyaniline-TiO_2 Nanotube for Surface Plasmon Resonance Enhanced Photoelectrochemical Biosensing

Jie Zhu[a], Xiaohe Huo[a], Xiaoqiang Liu[a*] and Huangxian Ju[b*]

[a] *Institute of Environmental and Analytical Sciences, College of Chemistry and Chemical Engineering, Henan University, Kaifeng, Henan Province, 475004, P.R. China*

[b] *State Key Laboratory of Analytical Chemistry for Life Science, Department of Chemistry, Nanjing University, Nanjing 210023, P.R. China*

* Corresponding author. Phone/Fax: +86-25-83593593, E-mail: liuxiaoqiang@henu.edu.cn; hxju@nju.edu.cn

ABSTRACT: A novel ternary composite composed of TiO_2 nanotubes (TiONTs), polyaniline (PANI) and gold nanoparticles (GNPs) was prepared for photoelectrochemical (PEC) biosensing. PANI was initially coated on TiONTs with an oxidative polymerization method, and 12-phosphotungstic acid was then used as a highly localized photoactive reducing agent to deposit GNPs on TiONT-PANI. The morphology and composition of the composite were characterized by various spectroscopic and microscopic methods. Electrochemical impedance spectroscopy was also conducted to demonstrate the excellent electrical conductivity of the composite. A PEC biosensor was fabricated by immobilizing a mixture of lactate dehydrogenase and the composite onto ITO electrodes, which regenerated nicotinamide adenine dinucleotide (NAD^+) to complete the enzymatic cycle and led to an improved method for PEC detection of lactate. Due to the surface plasmon resonance enhanced effect of GNPs, the electrochromic performance of PANI, excellent conductivity and biocompatibility of the composite, this method showed the dynamic range of 0.5 to 210 μM, sensitivity of 0.0401 μA μM^{-1} and the detection limit of 0.15 μM.

Keywords: *Photoelectrochemical biosensing; Surface plasmon resonance enhanced effect; Nanoparticle composite; TiO_2 nanotubes; 12-Phosphotungstic acid; Lactate dehydrogenase*

■ INTRODUCTION

The photoelectrochemical (PEC) sensing techniques have recently achieved dramatic progress in the detection of various biological and biochemical targets such as antigens,[1] nucleic acids,[2] enzymes,[3] enzyme substrates[4] and some other chemicals.[5] By integrating the traditional electrochemical method with the optical technique, the PEC based sensing techniques are able to maintain the advantages of both methods and minimize their shortcomings, resulting in the improved signal-to-noise ratio and sensitivity compared with the individual techniques.[4, 5] In particular, the PEC biosensors based on photoactive semiconducting nano-materials have shown superior performance to the conventional PEC sensors due to the reaction between the photo-generated holes from the photoactive semiconductors and the bio-catalyzed products. This reaction can retard the recombination between the photo-generated charges and thus enhance the photocurrent at PEC biosensor.[6, 7] For example, a BiOI nanoflakes/TiO_2 nanoparticles composite was prepared as the photoelectrode, on which acetylcholine esterase (AChE) antibody was immobilized for binding AChE to catalyze the conversion of acetylthiocholine to thiocholine.[4] Then thiocholine acted as a sacrificial electron donor to react with photo-excited holes, which could increase the photocurrents significantly.

TiO_2 nano-materials are the most promising and effective materials in PEC biosensing attributing to their excellent biocompatibility, chemical and mechanical stability, strong UV-Vis absorption and low cost.[8, 9] They have been used to prepare different types of PEC sensors or construct the detection methods for many biochemical and biological analytes including immunoglobulin G,[10] H_2O_2,[11] adenosine,[12] glucose,[13] and antigen.[14] However, the application of TiO_2 nano-materials in PEC sensing is always limited by their wide band gap, poor electrical conductivity and fast recombination of the photo-generated charges, which

significantly lower the photo-energy conversion efficiency and the sensitivity of the PEC sensors fabricated with TiO_2.[15-17] To minimize these handicaps, TiO_2 nano-materials were doped with various metal or nonmetal elements to obtain the composites with improved PEC properties.[17, 18] For example, hemin and IrO_2 nanoparticles have been co-deposited on TiO_2 nano-wires to enhance the light absorption and charge separation, and the PEC sensor based on this composite can sensitively detect glutathione in both buffer and cell extracts.[19]

As the most extensively studied conducting polymer, polyaniline (PANI) was widely used in the construction of electrochemical sensors due to its tunable electrical conductivity, reversible protonic dopability, redox reversibility, high environmental stability and easy preparation.[20, 21] Recently, PANI has demonstrated its feasibility as an active component in many PEC devices (e.g. solar cells) by exhibiting its unique electrical and optical properties such as charge storage capacity, electron trapping capability and photoelectric conversion performance.[22] For instance, the electrochromic performance of PANI can enhance the light absorption at visible region, hence producing more photo-generated electrons.[23] In addition, the conjugation structure of PANI molecules can capture more photo-excited electrons, retarding the recombination between photo-generated charge. Accordingly, modifying TiO_2 with PANI is an effective strategy to improve the photo-catalytic performance and shift the spectral absorption toward visible region.[24] For example, Li and coworkers prepared a PANI/TiO_2 nanoparticle composite, which displayed an improved photocatalytic activity than the pristine TiO_2.[24] Similarly, it is expected that the PEC performance of TiO_2 nano-materials can be obviously enhanced by combining PANI with TiO_2. More interestingly, PANI can also facilitate the deposition of GNPs on TNTs by attracting negative charged $AuCl_4^-$ on protonated secondary amines of PANI.[25] Furthermore, the highly conductive emeraldine salt PANI is able to improve the conductivity of TNTs.[26]

In the past few years, gold nanoparticles (GNPs) have frequently been applied in

electrochemical biosensors ascribing to their biocompatibility, large surface area, chemical stability, ease of preparation, and excellent electronic and optical properties etc.[27-29] More importantly, noble metal nanoparticles (Au, Pt and Pd) exhibited a surface plasmon resonance (SPR) effect during the photo-catalytic or PEC process, which can substantially increase the light absorption, enhance the charge separation and thus improve the photo-catalytic or PEC performance.[8, 30] Therefore, incorporating noble metal nanoparticles with wide band gap semiconductors such as TiO_2 can effectively enhance the PEC conversion efficiency of these semiconductors. For example, a GNP-decorated TiO_2 nanowire modified sensor has been developed for the detection of cholera toxin subunit B.[9] The SPR enhancement of GNP/TiO_2 nanowire composite produces an electrochemical field amplification effect, leading to a 100% increase of photocurrent density.

Determination of L-lactate in real samples can provide key information in the clinical diagnostics, medicine validation, and food analysis.[31, 33] Therefore, various electrochemical biosensors have been developed for the accurate and fast detection of lactate.[32, 33] However, these biosensors relied on the electrochemical oxidation of reduced nicotinamide adenine dinucleotide (NADH) to generate detection signals, which may be negatively affected by the high overpotential and electrode fouling.[33] Accordingly, a new method should be designed for the highly efficient conversion of NADH to nicotinamide adenine dinucleotide (NAD^+) to improve the lactate determination.

In this work, a novel functional composite composed of TiONTs, PANI and GNPs was synthesized following a procedure described by Scheme 1(A). Briefly, aniline was initially polymerized on TiONTs by an oxidative polymerization method. 12-Phosphotungstic acid (PTA; $PW_{12}O_{40}^{3-}$) was then modified on PANI-TiONT surface, and the photo-chemically reduced PTA acted as a localized reducing agent for deposition of GNPs on PANI-TiONT. By immobilizing lactate dehydrogenase (LDH) and NAD^+ on the composite modified ITO

electrode, a PEC biosensor for L-lactate was developed. Through integrating the SPR effect of GNP and the excellent PEC performance of PANI, the ternary composite transformed NADH back to NAD^+ in a highly efficient way to satisfy the LDH catalytic circle, improving the biosensor performance for detection of lactate.

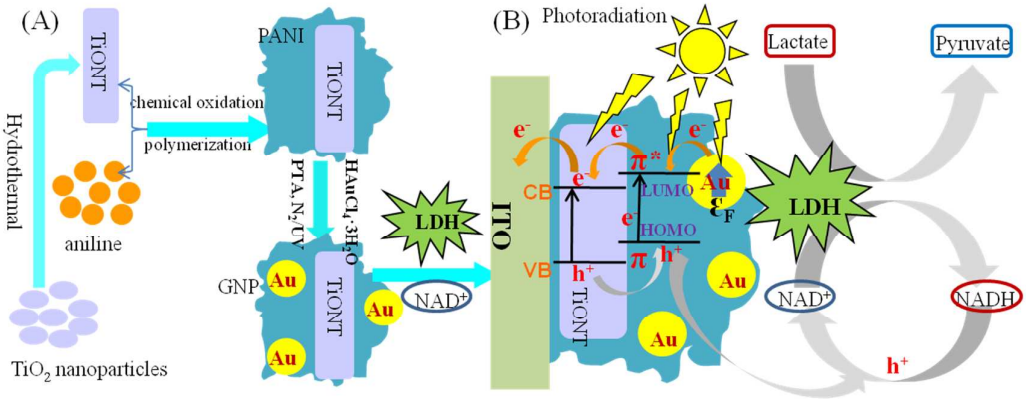

Scheme 1. (A) Schematic illustration for preparation of TiONT-PANI-GNP ternary composite, and (B) SPR-enhanced PEC detection of lactate at TiONT-PANI-GNP|LDH|NAD^+|ITO coupling with PEC coenzyme regeneration.

■ EXPERIMENTAL SECTION

Materials and Reagents. Aniline monomer (99.5% purity) and ammonium persulfate (98%) were purchased from J&K Scientific Ltd., Beijing, China. TiO_2 nanoparticles (P25) were obtained from Tianjin Chemical Reagent Co. Ltd., China. LDH, β-NAD^+ hydrate, NADH, sodium L-lactate, Nafion, ethylene diamine tetraacetic acid (EDTA), $HAuCl_4 \cdot 3H_2O$ and PTA were purchased from Sigma-Aldrich, USA. All other chemicals were of analytical grade and used without further purification. All solutions were prepared in Milli-Q ultrapure water. Potassium phosphate buffer (0.1 M, pH 7.4) was prepared and used as a supporting electrolyte.

Apparatus. PEC measurements were performed in a Quartz glass PEC cell, which was

designed by our lab and fabricated by Gaozhiruilian Co. Ltd., Wuhan, China. Philips tubular ultraviolet low-pressure 16-W mercury lamps were purchased from Philips Lighting B.V., The Netherlands. A Xe lamp equipped with visible light monochromator (CEL-HXUV 300) (Beijing AULTT, China) was used as the irradiation source. Electrochemical and PEC measurements were performed using a CHI630D electrochemical workstation (Shanghai CH Instruments, China). Indium tin oxide (ITO) electrodes were ordered from Wuhan lattice solar energy technology. Ltd., China. UV-Vis spectra were taken by a Hitachi U-4100 UV-Vis-Nir Spectrophotometer (HITACHI, Japan). Electrochemical impedance spectroscopy was obtained at an IM6ex electrochemical workstation (Zahner, Germany). The morphology and chemical composition of the nano-materials were characterized by transmission electron microscopy (TEM, Tecnai G2 20 USA), X-ray diffraction (XRD, Bruker D8 Advance, Germany) with Cu Kα radiation, and Fourier transform infrared spectroscopy (FT-IR, Nicolet 170, USA).

Preparation of Nanomaterials. TiONTs were prepared by initially pouring a mixture of 0.6 g P25 and 120 mL (10 M) NaOH aqueous solution to a Teflon-lined autoclave. After hydrothermal reaction at 120ºC for 48 hours, the white crude product was collected and washed with 0.1 M HCl three times, then neutralized with Milli-Q water to pH=7. Afterward, the product was centrifuged and the precipitation was dried in a 60°C oven for 2 hours and ground to powder.

The PANI-TiONT was synthesised as follows: initially 0.3 g TiONTs, 3.24 mL aniline hydrochloride solution (0.1 M) and 10 mL HCl solution (0.1 M) were mixed in a reaction vessel placed in an ice bath and the mixture was stirred for 0.5 h to obtain a uniform suspension. Next, 3.24 mL ammonium persulfate solution (0.1 M) was dropwise added to the mixture over 2-hour duration. The mixture was allowed to react

in an ice bath for another 3 hours before being stored at room temperature overnight. On the next day, the product was repeatedly washed with Milli-Q water until pH value was adjusted to ~7. Finally, the product was dried in a 60°C oven before it was ground to powder.

For preparing the TiONT-PANI-GNP composite, 20 mg PANI coated TiONT was dispersed in 20 mL PTA aqueous solution (10 mM) and the dispersion was mechanically stirred overnight. The product was then centrifuged and washed with Milli-Q water to remove the unattached PTA molecules. Next, 4 mL PTA-modified TiONT-PANI dispersion was mixed with 1 mL propan-2-ol in a quartz cell, which was purged with N_2 gas for 15 min. Then the mixture in the quartz cell was illuminated by four UV lamps (16 W, λex = 253 nm) for 4 h to photo-reduce PTA on the TiONT-PANI composite. The color of the mixture solution changed from dark green to brown at the end of the illumination. Afterward, 5 mL $HAuCl_4$ solution (1 mM) was added in the mixture and the solution was left untouched for 2 hours. Finally, the suspension was centrifuged to obtain TiONT-PANI-GNP composite and the composite was dried in oven at 60°C.

Preparation of Nanomaterial Modified GCE. 20 mg nanomaterial was dispersed in 300 μL PBS (0.1 M, pH 7.4) solution containing 0.5 wt% Nafion and the mixture was shaken in a thermostat oscillator at 4°C for 4 hours. Afterwards, 4 μL of the mixture was applied on a polished and cleaned GCE and dried in air. TiONT-PANI-GNP|LDH|NAD^+|GCE was fabricated using the same procedure except that 20 mg TiONT-PANI-GNP was dispersed in 300 μL PBS (0.1 M, pH 7.4) solution containing 7 mg mL^{-1} LDH, 15 mM NAD^+ and 0.5 wt% Nafion.

Preparation of PEC Biosensors. An ITO electrode was firstly cleaned with NaOH (1 M) and H_2O_2 (30%), then washed by acetone, alcohol and Milli-Q water successively under

sonification and dried at room temperature. Meanwhile, 20 mg TiONT-PANI-GNP was dispersed in 300 μL PBS (0.1 M, pH 7.4) solution containing 7 mg mL^{-1} LDH, 15 mM NAD^+ and 0.5 wt% Nafion. Subsequently, the mixture was shaken in a thermostat oscillator at 4°C for 4 hours, and 50 μL of the mixture was coated on the cleaned ITO electrode. The PEC biosensor was dried in refrigerator at 4°C overnight.

PEC Assay Procedure. PEC test was conducted in a quartz cell with a three-electrode system consisting of an ITO working electrode, a platinum wire auxiliary electrode, and a Ag|AgCl (3.0 M KCl) reference electrode. A Xe lamp equipped with a monochromator which only allows visible light to pass through was used as a light source to irradiate the ITO electrode in a homemade dark box. After the background photocurrent became stable, the PEC response was recorded.

■ RESULTS AND DISCUSSION

Characterization of Composite. As shown in Figure 1A, TiONT did not exhibit any obvious absorption peak between 300 and 900 nm except the typical absorption peak at ~283 nm (curve a), which is consistent with the previous report.[34] Curve b displayed two absorption bands centred at ~360 and 440, ascribing to the л-л* and polaron-л* transitions of ES-PANI.[35] TiONT-GNP (curve d) and TiONT-PANI-GNP (curve e) showed the plasmon resonance peak of pure GNPs (curve c) at ~516 nm despite of some minor peak position shift.[30] The SPR peak position shift may be induced by the strong interaction of GNPs with TiONT and PANI. The existence of localized SPR band in both binary (at ~524 nm, curve d) and ternary composites (at ~530 nm, curve e) indicated that TiONTs or PANI could not interfere with the plasmon resonance of the GNPs. The characteristic peak of TiONTs moved from 285

nm to 291 nm after deposition of GNPs on TiONTs (curve d). Most importantly, the typical absorption band attributed to the л-л* transition of PANI at ~360 nm, the characteristic peak of TiONTs at ~290 nm and the SPR peak of GNPs at ~530 nm were all observed on curve e, demonstrating the successful formation of ternary composite.[36]

The corresponding characteristic X-ray diffraction patterns of TiONTs, PANI, TiONT-PANI and TiONT-PANI-GNP were shown in Figure 1B. Curve a showed the diffraction peaks at 2θ of 9.6°, 24.8°, 28.4° and 48.7°, which were assigned to the (200), (110), (600) and (020) crystal planes of orthorhombic TiO_2 nanotubes, respectively.[37] PANI exhibited four typical peaks at approximately 9.3°, 15.0°, 21.0°, and 25.6° (curve b), assigning to the respective (001), (010), (100) and (110) crystal planes of emeraldine salt PANI (ES-PANI).[38] ES-PANI possesses good electrical conductivity,[26] which is a desirable character for the development of electrochemical and PEC biosensors. The XRD peaks of ES-PANI along with the typical peaks of TiONTs were observed in the XRD pattern of TiONT-PANI (curve c), indicating that PANI was coated on TiONT. However, the intensity of the PANI peaks attributed to the (010), (100) crystal planes declined significantly in TiONT-PANI and the PANI peak at 25.6° was overlapped with the TiONT peak at 24.8°. It was also noticed that the 2θ of the peaks attributed to the PANI crystal planes had minor shift after the formation of TiONT-PANI composite, which is probably due to the crystal form change caused by the strong interaction between PANI and TiONTs. In addition to the typical peaks belonging to PANI and TiONT, curve d exhibited some new XRD peaks at ~38.6°, 44.8°, 64.9° and 77.8° ascribing to the (110), (200), (220) and (311)

reflections of gold nanoparticles,[39] which indicated that GNPs were deposited on TiONT-PANI to form a ternary composite.

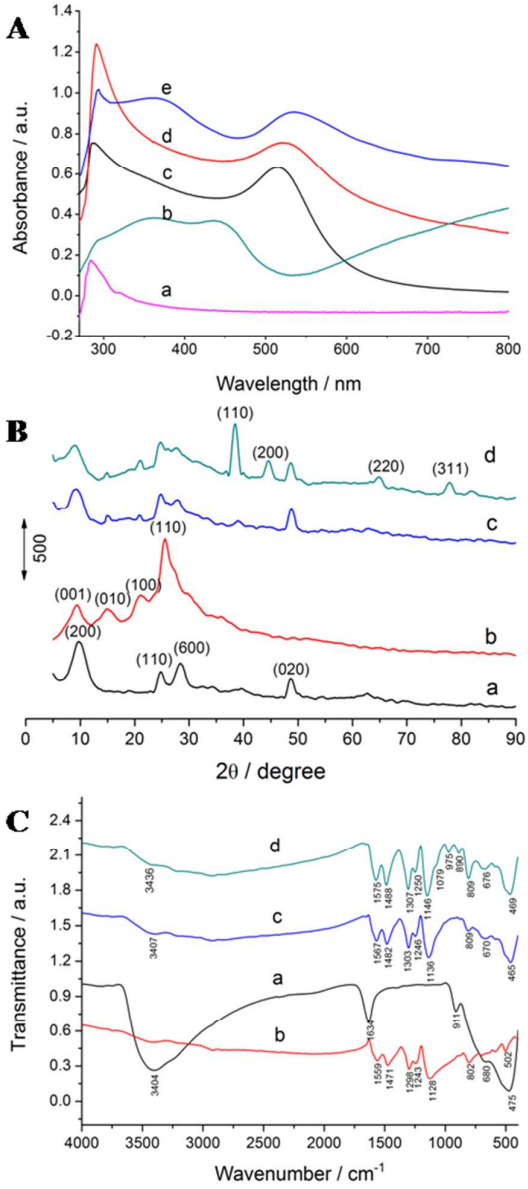

Figure 1. (A) UV-Vis spectra of (a) TiONTs, (b) PANI, (c) GNPs, (d) TiONT-GNP and (e) TiONT-PANI-GNP composite; (B) XRD patterns of (a) TiONTs, (b) PANI, (c) TiONT-PANI and (d) TiONT-PANI-GNP composite; (C) FT-IR spectra of (a) TiONTs, (b) PANI, (c) TiONT-PANI and (d) TiONT-PANI-GNP composite.

FT-IR spectra of TiONTs, PANI, TiONT-PANI and TiONT-PANI-GNP were acquired to investigate the structural information of these materials (Figure 1C). The broad absorption of TiONTs centred at 3404 cm^{-1} (curve a) was ascribed to the O-H stretching vibration arising from the TiONT surface hydroxyl.[40] In addition, the Ti–O stretching and Ti–O–Ti bridging vibration could be represented by two absorption bands at ~680 and ~475 cm^{-1} respectively, which are characteristic absorptions of TiO_2 nanomaterials.[41] The spectrum of PANI displayed three peaks at 1298, 1128 and 802 cm^{-1} corresponding to the C–N stretching of the secondary aromatic amine, the N=Q=N (Q represents the quinoid ring) stretching and the aromatic C–H out-of-plane bending vibration, respectively (curve b).[41, 42] Other two peaks ascribing to C=C stretching vibration of quinoid and benzenoid rings were also observed at 1559 cm^{-1} and 1471 cm^{-1}.[43] Furthermore, the peak at 1243 cm^{-1} attributed to $C–N^{+\bullet}$ stretching vibration indicated that PANI produced by the oxidation polymerisation method was emeraldine salt, which is highly conductive.[35] More importantly, TiONT-PANI exhibited the characteristic FT-IR bands of both PANI (700-1600 cm^{-1}) and TiO_2 nanomaterials (400-700 cm^{-1}) (curve c), demonstrating that the PANI-TiONT was successfully formed. It is also noticed that the characteristic PANI absorption peaks at 1559, 1471, 1298 and 1128 cm^{-1} shifted to 1567, 1482, 1303 and 1136 cm^{-1} respectively, which was induced by the strong bonding formed between the nitrogen atoms on PANI and the oxygen atoms on TiONTs.[44] The strong bonding restricted the chain vibration of PANI, which likely moved the vibration of PANI to higher wavenumbers.[34] The deposition of GNPs on TiONT-PANI resulted in further positive movement of the PANI absorption bands due to the strong interaction between GNPs and PANI (curve d). Interestingly, although GNPs did not produce any typical FT-IR

absorption, three characteristics bands at 1079, 975 and 890 cm^{-1} attributable to the chemical bonds between tungsten atoms, oxygen atoms and phosphorus atom (P-O_a, W-O_d and W-O_b-W) in PTA were observed.[45] These characteristic bands could be used as the proof of successful absorption of PTA on TiONTs by mechanical stirring. The PTA molecules on TiONTs were then photo-reduced to become the reducing agent for depositing GNPs on PANI-TiONT.

The TEM photo of TiONTs showed some well-separated tubiform nanostructures with a mean diameter of ~5-8 nm and length of a few hundred nm (Figure 2a), which were the typical morphological features of TiO_2 nanotubes.[29, 46] While the TEM photo of PANI showed dark crystalline grains embedded in semitransparent amorphous structure (Figure 2b), demonstrating the partial crystallinity of PANI.[47] In another word, PANI is a heterogeneous system with a crystalline phase dispersed in an amorphous region.[48] The partial crystallinity of PANI was attributed to the electrostatic attraction between the molecular chains in HCl doped-PANI.[47] After polymerization of aniline in the presence of TiONTs, semitransparent PANI was coated on TiONTs surface (Figure 2c).[49] In addition, TiONTs were not separated from each other anymore because PANI polymer bundled the TiO_2 nanotubes together. The TEM photo of TiONT-PANI-GNP showed a lot of dense dark particles on the surface of TiO_2 bundles (Figure 2d), indicating the successful deposition of GNPs on TiONT-PANI composite through photo-reduced PTA. From the magnified TEM image (inset in Figure 2d), the average particle size of GNPs was estimated to be 10-14 nm. From above TEM photos, intimate contact could be observed among TiONT, PANI and GNPs, which would facilitate the electron transfer within the ternary composite and improve the separation of photo-generated charges.

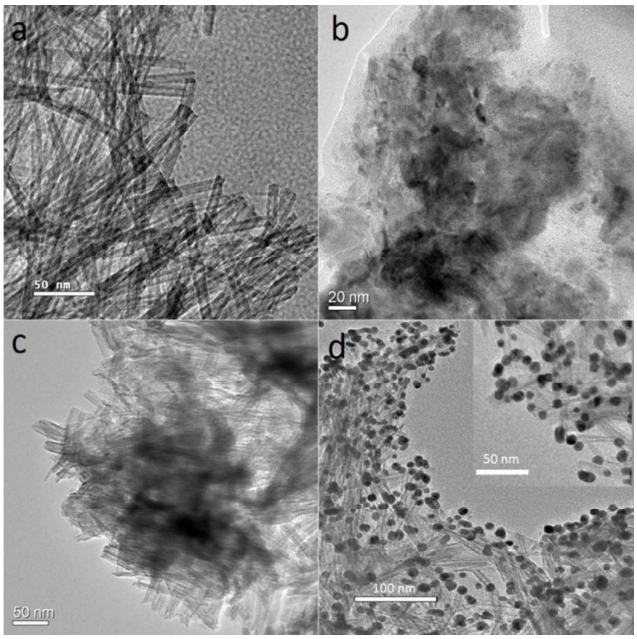

Figure 2. TEM images of (a) TiONTs, (b) PANI, (c) TiONT-PANI and (d) TiONT-PANI-GNP composite.

The electrical conductivity of the nanomaterials was evaluated with electrochemical impedance spectroscopy (EIS). Impedance measurements was performed in 0.1 M KCl solution containing 5.0 mM $[Fe(CN)_6]^{3-}$/$[Fe(CN)_6]^{4-}$ at a DC potential of 0.21 V. An alternating voltage of 5 mV was superimposed on the applied DC potential. Nyquist plots were recorded over a frequency range from 100 kHz-0.1 Hz (Figure 3). The quantity of the nano-materials immobilized on all the electrodes was identical in this test. For each curve, a semicircle was obtained in the higher frequency region and a straight line was observed in the lower frequency region, indicating a mixed electron transfer and diffusion control mechanism for the $[Fe(CN)_6]^{3-/4-}$ reaction at the electrode surface. The semicircle diameter is proportional to the electron transfer resistance (R_{et}) at surface of the electrode.[50] As expected, the Nyquist plot of the bare electrode exhibited a straight line with the smallest semicircle in these four curves,

implying a nearly complete diffusion control process (curve a). Noticeably, the semicircle diameters for TiONT, TiONT-PANI and TiONT-PANI-GNP modified electrode decreased in accordance with the sequence (curves b-d), indicating the decreasing R_{et}. These results strongly supported that both PANI and GNPs could significantly enhance electrical conductivity of the TiONT-PANI-GNP composite, which will benefit the performance of the electrochemical or PEC sensors using the ternary composite as sensor scaffold.

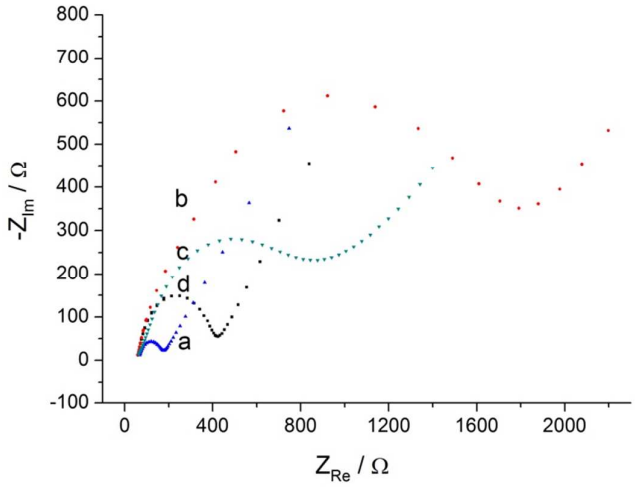

Figure 3. Nyquist plots of 5.0 mM $[Fe(CN)_6]^{3-}$/$[Fe(CN)_6]^{4-}$ at (a) bare, (b) TiONT, (c) TiONT-PANI and (d) TiONT-PANI-GNP modified GCE in 0.1 M KCl at a DC potential of 0.21 V.

Voltammetric Characterization of Electrochemical Biosensor. In the absence of lactate, both TiONT-PANI-GNP and TiONT-PANI-GNP|LDH|NAD^+ modified GCE showed flat and featureless voltammograms (Figure 4, curves a and c), indicating that the ternary composite did not produce any electrochemical interference. Because the weight of PANI in the composite was less than 10% and TiONT was electrochemically inert, the redox currents of PANI were so small that they were covered by the charging current of the composite

modified electrode. In addition, TiONT-PANI-GNP modified GCE did not show any obvious electrochemical signal in the presence of 5 mM L-lactate (Figure 4, curve b), meaning that lactate could not be oxidized or reduced electrochemically within a potential range from 0 to 0.8 V. More importantly, a distinct anodic peak (versus Ag/AgCl) was observed at ~0.49 V at TiONT-PANI-GNP|LDH|NAD^+ modified GCE in the presence of 5 mM lactate (Figure 4, curve d), which demonstrated the high catalytic activity of LDH in the ternary composite. The catalytic mechanism of LDH to lactate under the aid of coenzyme-NAD^+ can be described by the following equation (1) and (2). Briefly, LDH initially catalyzed the conversion of lactate to pyruvate with the help of NAD^+, which was simultaneously reduced to NADH. Owing to the excellent electrochemical properties of TiONT-PANI-GNP, NADH could be oxidized back to NAD^+ at a moderate potential of ~0.49 V (versus Ag/AgCl) to provide electrochemical signal for lactate detection.

$$\text{Lactate} + NAD^+ \xrightarrow{\text{LDH}} \text{Pyruvate} + \text{NADH} + H^+ \quad (1)$$

$$\text{NADH} - 2e^- \xrightarrow{\text{electrochemical oxidation}} NAD^+ + H^+ \quad (2)$$

The voltammetric results in Figure 4 confirmed that the ternary composite was a feasible immobilization material for the development of electrochemical and PEC biosensors. However, the current for NADH oxidation was relatively low at a high concentration of lactate (5 mM), indicating the low sensitivity of the electrochemical biosensor for detecting lactate.[32] Furthermore, the electrochemical oxidation regeneration of NAD^+ could be slow and incomplete, resulting in poor performance of the electrochemical lactate biosensor. Therefore, it is meaningful and highly necessary to develop a new type of biosensor with improved analytical performance.

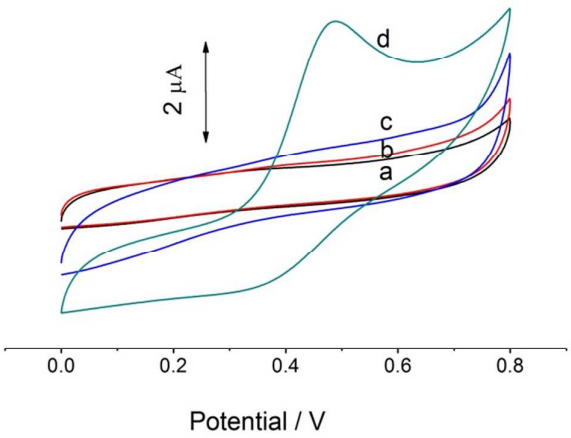

Figure 4 Cyclic voltammograms of TiONT-PANI-GNP|GCE in absence (a) and presence (b) of 5 mM L-lactate, and TiONT-PANI-GNP|LDH|NAD^+|GCE in absence (c) and presence (d) of 5 mM L-lactate in 0.1 M PBS (pH 7.4) at a scan rate of 50 mV s^{-1}.

PEC Characterization of Modified ITO. The PEC performance of different modified ITO electrodes was evaluated by monitoring the photocurrents produced by illuminating the electrodes with intermittent visible incident light (Figure 5A). The photocurrent at TiONT-PANI modified ITO (curve b) was ~53% larger than that at TiONT modified ITO (curve a), which could be attributed to the electrochromic performance, electron capture capability and good conductivity of PANI. Specifically, the electrochromic character of PANI improved the visible light absorption and enhanced the charge seperation.[23] In addition, the good electrical conductivity of PANI facilitated the movement of photo-excited electrons from TiONTs to ITO electrode, preventing the recombination of the photo-generated charges. Notably, TiONT-PANI-GNP modified ITO (curve c) showed a ~79% higher photocurrent than PANI-TiONT modified ITO (curve b) due to the SPR effect of GNPs, which increased the light absorption, enhanced the charge separation, and thus improved the PEC

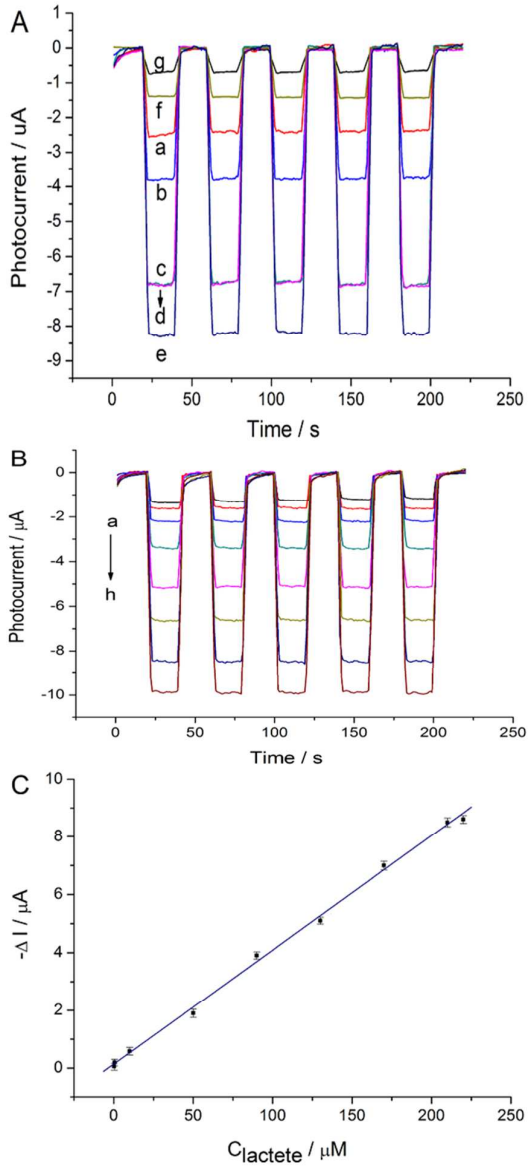

Figure 5 (A) Photocurrents obtained at (a) TiONT|ITO, (b) TiONT-PANI|ITO, (c) TiONT-PANI-GNP|ITO, (d) TiONT-PANI-GNP|ITO in presence of 100 μM L-lactate, (e) TiONT-PANI-GNP|ITO in presence of 100 μM NADH, (f) TiONT-PANI-GNP|LDH|NAD^+|ITO and (g) TiONT-PANI|LDH|NAD^+|ITO in absence of L-lactate. (B) Photocurrents obtained at TiONT-PANI-GNP|LDH|NAD^+|ITO with L-lactate concentrations of 0, 0.5, 10, 50, 90, 130, 170 and 210 μM (a-h) at 0.2 V; (C) Plot of photocurrent vs L-lactate concentration.

conversion efficiency of the semiconductors.[8, 30] In the presence of 100 μM lactate, the photocurrent of TiONT-PANI-GNP modified ITO did not change (curve d), which demonstrated that the photo-excited holes were not able to oxidize lactate directly. On the contrary, TiONT-PANI-GNP modified ITO displayed strong oxidation ability towards NADH, which resulted in a significant photocurrent enhancement (curve e). This photocurrent enhancement indicated that the photo-excited holes could efficiently regenerate NAD^+ from NADH to complete the enzymatic cycle as shown in equation (1) and (2), which was an essential requirement for the development of a LDH-based biosensor. Noticeably, TiONT-PANI-GNP|LDH|NAD^+ modified ITO (curve f) displayed the lowest photocurrent among all the modified electrodes owing to the steric hindrance of the enzyme molecules on ITO. The steric hindrance of enzymes retarded the moving of photo-generated electrons to ITO and thus increased their recombination with the holes.[32] Even though, the PEC currents at TiONT-PANI-GNP|LDH|NAD^+|ITO (curve f) are still larger than those at TiONT-PANI|LDH|NAD+|ITO (curve g), offering another proof for SPR enhanced effect of GNPs. The linear scan voltammetric curves of TiONT-PANI-GNP|ITO and TiONT-PANI-GNP|LDH|NAD^+|ITO under the illumination further confirmed these results (Figure S1, Supporting Information).

SPR-enhanced PEC Detection of Lactate at TiONT-PANI-GNP|LDH|NAD^+|ITO. The PEC reaction mechanism of L-lactate at TiONT-PANI-GNP|LDH|NAD^+ modified ITO was displayed in Scheme 1B. During the light irradiation, the SPR-excited electrons on GNPs were firstly injected into the π* orbit of PANI. At the same time, the electrons at PANI π orbit were also photo-excited and jumped to the π* orbit through light absorption. Because the π* orbit position of PANI is higher than the conduction band (CB) and valence band (VB) positions of TiO_2,[24, 51] the electrons at the π* orbit were rapidly transported into the CB of

TiO_2. Eventually all the photo-excited electrons were attracted to ITO by the applied potential (0.2 V) to produce enlarged photocurrent. In addition, LDH catalysed the transformation of lactate to pyruvate with the aid of NAD^+, which was converted to NADH simultaneously. Afterward, NADH was oxidized back to NAD^+ by the photo-generated holes at PANI π orbit, which were transferred from the VB TiO_2 during the illumination. The increase of lactate concentration in the test solution produced more NADH, which would consume more photo-excited holes and therefore generate larger photocurrent for quantitative determination of lactate.

Some important experimental parameters such as pH value of test solution, applied potential, LDH and NAD^+ concentrations were optimized before the final performance evaluation. As shown in Figure S2 in Supporting Information, the optimal concentrations of LDH and NAD^+ in TiONT-PANI-GNP dispersion were 7 mg mL^{-1} and 15 mM, and the optimal pH value was 7.4. Besides, the photocurrent enhanced noticeably with increasing applied potential up to 0.2 V. To minimize the oxidation of some possible interfering substances and NADH, an applied potential of 0.2 V was used in the subsequent PEC experiments. At the optimum experimental conditions, the photocurrent response of TiONT-PANI-GNP|LDH|NAD^+ modified ITO enhanced with increasing lactate concentration (Figure 5B). The calibration curve could be constructed by plotting $-\Delta I$ ($\Delta I = I - I_0$, I represents the photocurrent obtained in the presence of lactate and I_0 is the blank photocurrent.) versus lactate concentration (Figure 5C). A dynamic range between 0.5 and 210 μM was obtained from the calibration plot with a correlation coefficient of 0.996. The sensitivity and detection limit were estimated to be 0.0401 μA μM^{-1} and 0.15 μM respectively. As displayed in Table 1, the analytical performance of TiONT-PANI-GNP|LDH|NAD^+ modified ITO showed superiority over most of the electrochemical biosensors, which is

attributed to the SPR enhanced PEC effect and synergistic effect of TiONT-PANI-GNP composite.

Table 1. Analytical performance of some electrochemical and PEC biosensors for L-lactate

LDH-based biosensors	Linear Range (μM)	Detection limit (μM)	Sensitivity (μA μM^{-1})	References
TiONT-PANI-GNP|LDH|NAD^+|ITO	0.5-210	0.15	0.0401	This work
TiONT-PANI|LDH|NAD^+|ITO	1-180	0.55	0.0185	This work
MWCNT-CHIT[d]-LDH	5-120	0.76	0.0083	32
pTTCA[c]/MWNT/LDH/NAD^+	5-90	1.0	0.0106	33
Sol–gel/PVA[a]-LDH/Au electrode	2-30	0.80	0.1040	52
Polysulfone/MWCNT/LDH/SPCE[b]	1-20	0.37	0.0073	53
Fe_3O_4/MWCNTs/LDH/NAD^+	50-500	5.0	0.0077	54
Nano-TiO_2 –LDH/GCE	1-20	0.4	0.0493	55
LDH/Graphite screen printing ink	20-200	10	0.0010	56

[a] polyvinyl alcohol; [b] screen-printed carbon electrode; [c] poly-5,2'-5',2"-terthiophene-3' -carboxylic acid; [d]chitosan

Precision, Stability, Interference Test and Real Sample Analysis. The precision, stability and practical application of the proposed biosensor were included in Supporting Information. The relative standard deviation (RSD) of the photocurrents at six biosensors was 4.9%, indicating an acceptable fabrication precision. Furthermore, 96.1%, 92.5% and 87.3% of the initial photocurrents were retained after the PEC biosensors were stored at 4 ºC for 1, 2 and 4 weeks, respectively. The selectivity of TiONT-PANI-GNP|LDH|NAD^+ modified ITO was evaluated through investigating the influence of some possible interfering substances including citrate, carbonate, fructose, sucrose, phenylalanine, arginine, glucose, ascorbic acid and uric acid on the determination of 20 μM lactate respectively. After 50 μM each of the above interfering substances was added into 20 μM lactate solution respectively,

the photocurrent at TiONT-PANI-GNP|LDH|NAD^+ modified ITO fluctuated ~2.1%, 2.7%, -1.7%, 1.8%, 2.9%, 1.5%, 3.8%, 4.4% and 3.1% compared to the photocurrents obtained before the addition of the interfering substances. The interference may be ascribed to the oxidation of the interfering substances by the photo-generated holes at the applied potential (0.2 V). However, the interfering signals are neglectable compared with the photocurrents produced by the LDH PEC biosensor. The average recoveries for the detection of lactate in serum and milk samples were obtained to be 98.2% and 96.9%, indicating the potential practical application of the PEC biosensor.

■ CONCLUSION

A ternary composite consisting of TiONTs, PANI and GNPs was synthesised and characterised by UV-Vis, XRD, FT-IR, TEM and EIS. The PEC and electrochemical results demonstrated that the catalytic capability of LDH could be well maintained in the ternary composite. The TiONT-PANI-GNP modified ITO electrode exhibited larger PEC response than TiONTs and TiONT-PANI modified ITO due to the SPR-enhanced effect of GNP and electrochromic performance of PANI. TiONT-PANI-GNP|LDH|NAD^+ modified ITO as the proposed PEC biosensor showed excellent analytical performance for the detection of L-lactate, ascribing to the extraordinary PEC properties and biocompatibility of the ternary composite. In addition, the n-type TiONTs and p-type PANI can form a p-n heterojunction, which could enlarge the separation of the photo-excited charge, retard their recombination, and further increase the photocurrent of the PEC biosensor.

■ ACKNOWLEDGMENTS

This work was financially supported by the Open Research Funding of State Key Laboratory of Analytical Chemistry for Life Science, Nanjing University (No. SKLACLS1409), National Natural Science Foundation of China (No. U1504215) and the Scientific Research Foundation for the Returned Overseas Chinese Scholars, Ministry of Education (Batch 46th).

■ AUTHOR INFORMATION

Corresponding Authors

*Phone/Fax: +86-25-83593593, e-mail: liuxiaoqiang@henu.edu.cn；hxju@nju.edu.cn

Notes

The authors declare no competing financial interest.

■ ASSOCIATED CONTENT

Supporting Information

Additional information as noted in text. This material is available free of charge via the Internet at http://pubs.acs.org.

Reduction of $AuCl_4^-$ to gold nanoparticles by PTA; linear scan voltammetric curves of TiONT-PANI-GNP|ITO and TiONT-PANI-GNP|LDH|NAD^+|ITO in both dark and light condition; optimization of preparation and detection conditions; precision, stability and real sample analysis.

■ REFERENCES

(1) Zeng, X.; Bao, J.; Han, M.; Tu, W.; Dai, Z. Quantum Dots Sensitized Titanium Dioxide Decorated Reduced Graphene Oxide for Visible Light Excited Photoelectrochemical Biosensing at a Low Potential. *Biosens. Bioelectron.* **2014**, *54*, 331-338.

(2) Willner, I.; Patolsky, F.; Wasserman, J. Photoelectrochemistry with Controlled DNA-Cross-Linked CdS Nanoparticle Arrays. *Angew. Chem., Int. Ed.* **2001**, *40*, 1861-1864.

(3) Tanne, J.; Schafer, D.; Khalid, W.; Parak, W. J.; Lisdat, F. Light-Controlled Bioelectrochemical Sensor Based on CdSe/ZnS Quantum Dots. *Anal. Chem.* **2011**, *83*, 7778-7785.

(4) Zhao, W.-W.; Shan, S.; Ma, Z.-Y.; Wan, L.-N.; Xu, J.-J.; Chen, H.-Y. Acetylcholine Esterase Antibodies on Bioi Nanoflakes/TiO_2 Nanoparticles Electrode: A Case of Application for General Photoelectrochemical Enzymatic Analysis. *Anal. Chem.* **2013**, *85*, 11686-11690.

(5) Li, H.; Li, J.; Xu, Q.; Hu, X. Poly(3-Hexylthiophene)/TiO_2 Nanoparticle-Functionalized Electrodes for Visible Light and Low Potential Photoelectrochemical Sensing of Organophosphorus Pesticide Chlopyrifos. *Anal. Chem.* **2011**, *83*, 9681-9686.

(6) Xia, L.; Song, J.; Xu, R.; Liu, D.; Dong, B.; Xu, L.; Song, H. Zinc Oxide Inverse Opal Electrodes Modified by Glucose Oxidase for Electrochemical and Photoelectrochemical Biosensor. *Biosens. Bioelectron.* **2014**, *59*, 350-357.

(7) Zhao, W.-W.; Yu, P.-P.; Xu, J.-J.; Chen, H.-Y. Ultrasensitive Photoelectrochemical Biosensing Based on Biocatalytic Deposition. *Electrochem. Commun.* **2011**, *13*, 495-497.

(8) Da, P.; Li, W.; Lin, X.; Wang, Y.; Tang, J.; Zheng, G. Surface Plasmon Resonance Enhanced Real-Time Photoelectrochemical Protein Sensing by Gold Nanoparticle-Decorated TiO_2 Nanowires. *Anal. Chem.* **2014**, *86*, 6633-6639.

(9) Wang, G.; Wang, H.; Ling, Y.; Tang, Y.; Yang, X.; Fitzmorris, R. C.; Wang, C.; Zhang, J. Z.; Li, Y. Hydrogen-Treated TiO_2 Nanowire Arrays for Photoelectrochemical Water Splitting. *Nano Lett.* **2011**, *11*, 3026-3033.

(10) Mun, K.-S.; Alvarez, S. D.; Choi, W.-Y.; Sailor, M. J. A Stable, Label-Free Optical Interferometric Biosensor Based on TiO_2 Nanotube Arrays. *ACS nano* **2010**, *4*, 2070-2076.

(11) Chen, D.; Zhang, H.; Li, X.; Li, J. Biofunctional Titania Nanotubes for Visible-Light-Activated Photoelectrochemical Biosensing. *Anal. Chem.* **2010**, *82*, 2253-2261.

(12) Tian, C.-Y.; Xu, J.-J.; Chen, H.-Y. A Novel Aptasensor for the Detection of Adenosine in Cancer Cells by Electrochemiluminescence of Nitrogen Doped TiO_2 Nanotubes. *Chem. Commun.* **2012**, *48*, 8234-8236.

(13) Wang, Y.; Tang, J.; Peng, Z.; Wang, Y.; Jia, D.; Kong, B.; Elzatahry, A. A.; Zhao, D.; Zheng, G. Fully Solar-Powered Photoelectrochemical Conversion for Simultaneous Energy Storage and Chemical Sensing. *Nano Lett.* **2014**, *14*, 3668-3673.

(14) Zhao, W.-W.; Ma, Z.-Y.; Yan, D.-Y.; Xu, J.-J.; Chen, H.-Y. In Situ Enzymatic Ascorbic Acid Production as Electron Donor for CdS Quantum Dots Equipped TiO_2 Nanotubes: A General and Efficient Approach for New Photoelectrochemical Immunoassay. *Anal. Chem.* **2012**, *84*, 10518-10521.

(15) Wender, H.; Feil, A. F.; Diaz, L. B.; Ribeiro, C. S.; Machado, G. J.; Migowski, P.; Weibel, D. E.; Dupont, J.; Teixeira, S. R. Self-Organized TiO_2 Nanotube Arrays: Synthesis by Anodization in an Ionic Liquid and Assessment of Photocatalytic Properties. *ACS Appl. Mater. Interfaces* **2011**, *3*, 1359-1365.

(16) Li, X.; Hou, Y.; Zhao, Q.; Chen, G. Synthesis and Photoinduced Charge-Transfer Properties of a $ZnFe_2O_4$-Sensitized TiO_2 Nanotube Array Electrode. *Langmuir* **2011**, *27*, 3113-3120.

(17) Hamedani, H. A.; Allam, N. K.; Garmestani, H.; El-Sayed, M. A. Electrochemical Fabrication of Strontium-Doped TiO_2 Nanotube Array Electrodes and Investigation of Their Photoelectrochemical Properties. *J. Phys. Chem. C* **2011**, *115*, 13480-13486.

(18) Gong, J.; Pu, W.; Yang, C.; Zhang, J. A Simple Electrochemical Oxidation Method to Prepare Highly Ordered Cr-Doped Titania Nanotube Arrays with Promoted Photoelectrochemical Property. *Electrochim. Acta* **2012**, *68*, 178-183.

(19) Tang, J.; Kong, B.; Wang, Y.; Xu, M.; Wang, Y.; Wu, H.; Zheng, G. Photoelectrochemical Detection of Glutathione by IrO_2-Hemin-TiO_2 Nanowire Arrays. *Nano Lett.* **2013**, *13*, 5350-5354.

(20) Kan, J.; Pan, X.; Chen, C. Polyaniline-Uricase Biosensor Prepared with Template Process. *Biosens. Bioelectron.* **2004**, *19*, 1635-1640.

(21) Tang, W.; Li, L.; Zeng, X. A Glucose Biosensor Based on the Synergistic Action of Nanometer-Sized TiO_2 and Polyaniline. *Talanta* **2015**, *131*, 417-423.

(22) Li, Q.; Wu, J.; Tang, Q.; Lan, Z.; Li, P.; Lin, J.; Fan, L. Application of Microporous Polyaniline Counter Electrode for Dye-Sensitized Solar Cells. *Electrochem. Commun.* **2008**, *10*, 1299-1302.

(23) Pud, A.; Ogurtsov, N.; Korzhenko, A.; Shapoval, G. Some Aspects of Preparation Methods and Properties of Polyaniline Blends and Composites with Organic Polymers. *Prog. Polym. Sci.* **2003**, *28*, 1701-1753.

(24) Li, X.; Wang, D.; Cheng, G.; Luo, Q.; An, J.; Wang, Y. Preparation of Polyaniline-Modified TiO_2 Nanoparticles and Their Photocatalytic Activity under Visible Light Illumination. *Appl. Catal., B* **2008**, *81*, 267-273.

(25) Liu, S.; Xu, H.; Ou, J.; Li, Z.; Yang, S.; Wang, J. A Feasible Approach to the Fabrication of Gold/Polyaniline Nanofiber Composites and Its Application as Electrocatalyst for Oxygen Reduction. *Mater. Chem. Phys.* **2012**, *132*, 500-504.

(26) Athawale, A. A.; Kulkarni, M. V.; Chabukswar, V. V. Studies on Chemically Synthesized Soluble Acrylic Acid Doped Polyaniline. *Mater. Chem. Phys.* **2002**, *73*, 106-110.

(27) Dequaire, M.; Degrand, C.; Limoges, B. An Electrochemical Metalloimmunoassay Based on a Colloidal Gold Label. *Anal. Chem.* **2000**, *72*, 5521-5528.

(28) Daniel, M.-C.; Astruc, D. Gold Nanoparticles: Assembly, Supramolecular Chemistry, Quantum-Size-Related Properties, and Applications toward Biology, Catalysis, and Nanotechnology. *Chem. Rev. (Washington, DC, U. S.)* **2004**, *104*, 293-346.

(29) Liu, X.; Zhang, J.; Liu, S.; Zhang, Q.; Liu, X.; Wong, D. K. Y. Gold Nanoparticle Encapsulated-Tubular TiO_2 Nanocluster as a Scaffold for Development of Thiolated Enzyme Biosensors. *Anal. Chem.* **2013**, *85*, 4350-4356.

(30) Zhuang, J.; Lai, W.; Xu, M.; Zhou, Q.; Tang, D. Plasmonic AuNP/G-C_3N_4 Nanohybrid-Based Photoelectrochemical Sensing Platform for Ultrasensitive Monitoring of Polynucleotide Kinase Activity Accompanying Dnazyme-Catalyzed Precipitation Amplification. *ACS Appl. Mater. Interfaces* **2015**, *7*, 8330-8338.

(31) Chaubey, A.; Gerard, M.; Singhal, R.; Singh, V. S.; Malhotra, B. D. Immobilization of Lactate Dehydrogenase on Electrochemically Prepared Polypyrrole-Polyvinylsulphonate Composite Films for Application to Lactate Biosensors. *Electrochim. Acta* **2001**, *46*, 723-729.

(32) Tsai, Y.-C.; Chen, S.-Y.; Liaw, H.-W. Immobilization of Lactate Dehydrogenase within Multiwalled Carbon Nanotube-Chitosan Nanocomposite for Application to Lactate Biosensors. *Sens. Actuators, B* **2007**, *125*, 474-481.

(33) Rahman, M. M.; Shiddiky, M. J. A.; Rahman, M. A.; Shim, Y.-B. A Lactate Biosensor Based on Lactate Dehydrogenase/Nictotinamide Adenine Dinucleotide (Oxidized Form) Immobilized on a Conducting Polymer/Multiwall Carbon Nanotube Composite Film. *Anal. Biochem.* **2009**, *384*, 159-165.

(34) Katoch, A.; Burkhart, M.; Hwang, T.; Kim, S. S. Synthesis of Polyaniline/TiO_2 Hybrid Nanoplates Via a Sol-Gel Chemical Method. *Chem. Eng. J.* **2012**, *192*, 262-268.

(35) Oh, M.; Kim, S. Synthesis and Electrochemical Analysis of Polyaniline/TiO_2 Composites Prepared with Various Molar Ratios between Aniline Monomer and Para-Toluenesulfonic Acid. *Electrochim. Acta* **2012**, *78*, 279-285.

(36) Kim, B.-S.; Lee, K.-T.; Huh, P.-H.; Lee, D.-H.; Jo, N.-J.; Lee, J.-O. In Situ Template Polymerization of Aniline on the Surface of Negatively Charged TiO_2 Nanoparticles. *Synth. Met* **2009**, *159*, 1369-1372.

(37) Zhang, M.; Jin, Z.; Zhang, J.; Guo, X.; Yang, J.; Li, W.; Wang, X.; Zhang, Z. Effect of Annealing Temperature on Morphology, Structure and Photocatalytic Behavior of Nanotubed $H_2Ti_2O_4(OH)_2$. *J. Mol. Catal. A: Chem.* **2004**, *217*, 203-210.

(38) Srivastava, S.; Kumar, S.; Singh, V. N.; Singh, M.; Vijay, Y. K. Synthesis and Characterization of TiO_2 Doped Polyaniline Composites for Hydrogen Gas Sensing. *Int. J. Hydrogen Energy* **2011**, *36*, 6343-6355.

(39) Paramasivam, I.; Macak, J. M.; Schmuki, P. Photocatalytic Activity of TiO_2 Nanotube Layers Loaded with Ag and Au Nanoparticles. *Electrochem. Commun.* **2008**, *10*, 71-75.

(40) Zhang, H.; Lv, X.; Li, Y.; Wang, Y.; Li, J. P25-Graphene Composite as a High Performance Photocatalyst. *ACS nano* **2009**, *4*, 380-386.

(41) Karim, M. R.; Yeum, J. H.; Lee, M. S.; Lim, K. T. Preparation of Conducting Polyaniline/TiO_2 Composite Submicron-Rods by the γ-Radiolysis Oxidative Polymerization Method. *React. Funct. Polym.* **2008**, *68*, 1371-1376.

(42) Karim, M. R.; Lim, K. T.; Lee, M. S.; Kim, K.; Yeum, J. H. Sulfonated Polyaniline-Titanium Dioxide Nanocomposites Synthesized by One-Pot UV-Curable Polymerization Method. *Synth. Met* **2009**, *159*, 209-213.

(43) Irimia-Vladu, M.; Marjanovic, N.; Vlad, A.; Ramil, A. M.; Hernandez-Sosa, G.; Schwoödiauer, R.; Bauer, S.; Sariciftci, N. S. Vacuum-Processed Polyaniline–C60 Organic Field Effect Transistors. *Adv. Mater.* **2008**, *20*, 3887-3892.

(44) Yavuz, A. G.; Gok, A. Preparation of TiO_2/PANI Composites in the Presence of Surfactants and Investigation of Electrical Properties. *Synth. Met.* **2007**, *157*, 235-242.

(45) Pearson, A.; Jani, H.; Kalantar-zadeh, K.; Bhargava, S. K.; Bansal, V. Gold Nanoparticle-Decorated Keggin Ions/TiO_2 Photococatalyst for Improved Solar Light Photocatalysis. *Langmuir* **2011**, *27*, 6661-6667.

(46) Liu, X.; Yan, R.; Zhang, J.; Zhu, J.; Wong, D. K. Y. Evaluation of a Carbon Nanotube-Titanate Nanotube Nanocomposite as an Electrochemical Biosensor Scaffold. *Biosens. Bioelectron.* **2015**, *66*, 208-215.

(47) Duan, Y.; Wu, G.; Li, X.; Ji, Z.; Liu, S.; Li, W. On the Correlation between Structural Characterization and Electromagnetic Properties of Doped Polyaniline. *Solid State Sci.* **2010**, *12*, 1374-1381.

(48) Belabed, C.; Abdi, A.; Benabdelghani, Z.; Rekhila, G.; Etxeberria, A.; Trari, M. Photoelectrochemical Properties of Doped Polyaniline: Application to Hydrogen Photoproduction. *Int. J. Hydrogen Energy* **2013**, *38*, 6593-6599.

(49) Yan, W.; Feng, X.; Chen, X.; Hou, W.; Zhu, J.-J. A Super Highly Sensitive Glucose Biosensor Based on Au Nanoparticles–AgCl@Polyaniline Hybrid Material. *Biosens. Bioelectron.* **2008**, *23*, 925-931.

(50) Liu, X.; Duckworth, P. A.; Wong, D. K. Y. Square Wave Voltammetry Versus Electrochemical Impedance Spectroscopy as a Rapid Detection Technique at Electrochemical Immunosensors. *Biosens. Bioelectron.* **2010**, *25*, 1467-1473.

(51) Zhang, H.; Zong, R.; Zhao, J.; Zhu, Y. Dramatic Visible Photocatalytic Degradation Performances Due to Synergetic Effect of TiO_2 with PANI. *Environ. Sci. Technol.* **2008**, *42*,

3803-3807.

(52) Di, J.; Cheng, J.; Xu, Q.; Zheng, H.; Zhuang, J.; Sun, Y.; Wang, K.; Mo, X.; Bi, S. Direct Electrochemistry of Lactate Dehydrogenase Immobilized on Silica Sol-Gel Modified Gold Electrode and Its Application. *Biosens. Bioelectron.* **2007**, *23*, 682-687.

(53) Pérez, S.; Sánchez, S.; Fàbregas, E. Enzymatic Strategies to Construct L-Lactate Biosensors Based on Polysulfone/Carbon Nanotubes Membranes. *Electroanalysis* **2012**, *24*, 967-974.

(54) Teymourian, H.; Salimi, A.; Hallaj, R. Low Potential Detection of NADH Based on Fe_3O_4 Nanoparticles/Multiwalled Carbon Nanotubes Composite: Fabrication of Integrated Dehydrogenase-Based Lactate Biosensor. *Biosens. Bioelectron.* **2012**, *33*, 60-68.

(55) Cheng, J.; Di, J.; Hong, J.; Yao, K.; Sun, Y.; Zhuang, J.; Xu, Q.; Zheng, H.; Bi, S. The Promotion Effect of Titania Nanoparticles on the Direct Electrochemistry of Lactate Dehydrogenase Sol-Gel Modified Gold Electrode. *Talanta* **2008**, *76*, 1065-1069.

(56) Avramescu, A.; Andreescu, S.; Noguer, T.; Bala, C.; Andreescu, D.; Marty, J.-L. Biosensors Designed for Environmental and Food Quality Control Based on Screen-Printed Graphite Electrodes with Different Configurations. *Anal. Bioanal. Chem.* **2002**, *374*, 25-32.

For Table of Contents Only